

# CoRoT and *Kepler* results: solar-like oscillators

S. Hekker

*Astronomical Institute 'Anton Pannekoek', University of Amsterdam, Science Park 904,  
1098 XH Amsterdam, The Netherlands*

*email: S.Hekker@uva.nl, tel: +31 20 525 7491, fax: +31 20 525 7484*

---

## Abstract

The space-borne observatories CoRoT (Convection Rotation and planetary Transits) and *Kepler* have provided photometric time series data of unprecedented precision for large numbers of stars. These data have revolutionized the fields of transiting exoplanets and asteroseismology. In this review some important asteroseismic results obtained using data from the CoRoT and *Kepler* space missions concerning stars that show solar-like oscillations are discussed. These results comprise, among others, measurements of the location of the base of the convection zone and helium second-ionization zone in main-sequence stars, the presence (or not) of core-helium burning in red-giant stars, as well as differential rotation in these stars.

### *Keywords:*

stars – main-sequence; stars – subgiants; stars – red giants; methods – asteroseismology

---

## 1. Introduction

2 Internal structure and compositions of stars as well as changes with evo-  
3 lution are broadly understood, but still have many challenges. Classical  
4 photometric and spectroscopic observations do not expose the stellar inte-  
5 rior due to the extreme opacity of stellar material which masks the internal  
6 structure from view. For the Sun the 5-minute acoustic oscillations allow  
7 us to peer inside the Sun (helioseismology) and provide much needed in-  
8 formation about the internal structure of the Sun and the relevant physical  
9 processes. We expect that oscillations in distant stars will also provide invalu-  
10 able probes of the internal structures of these stars. Oscillations in distant  
11 stars have been measured from the ground (e.g. Kjeldsen et al., 1995; Carrier

12 and Bourban, 2003; Bedding et al., 2004; Arentoft et al., 2008). However,  
13 these observations have limitations with respect to 1) the length and conti-  
14 nuity of the observations, 2) number of stars that can be observed (mostly  
15 relevant for spectroscopy, i.e. high-resolution spectrographs used for astero-  
16 seismology can only observe one star at a time, while in photometry many  
17 stars can be observed during one integration), and 3) the signal-to-noise ratio  
18 of the data (mostly relevant for photometry of low-amplitude oscillations).  
19 Space missions have distinct advantages that overcome most of these prob-  
20 lems. Therefore, dedicated space-missions have been developed. The first  
21 asteroseismic space mission MOST (Microvariability & Oscillations of STars,  
22 Matthews et al., 2000) was launched on June 30, 2003. MOST is a Canadian  
23 microsatellite observing bright stars (down to 6th magnitude) with a photo-  
24 metric precision of one part per million. In recent years major contributions  
25 in asteroseismology have come from the space missions CoRoT and *Kepler*.  
26 The CoRoT<sup>1</sup> (Convection Rotation and planetary Transits, Baglin et al.,  
27 2006) and *Kepler*<sup>2</sup> (Borucki et al., 2008) space missions have provided un-  
28 precedented photometric observations that allowed for many breakthroughs  
29 in both stellar and exoplanet research. Some details and characteristics of  
30 these missions are outlined here.

### 31 1.1. *CoRoT*

32 The objectives of the CoRoT mission were two-fold: discovering exoplan-  
33 ets down to super-earth radii and unravelling the internal structures of stars.  
34 To achieve this the CoRoT spacecraft was equipped with a 27 cm-diameter  
35 afocal telescope with an 8 square-degree field of view. To discover exoplan-  
36 ets via the transit method (when a planet crosses in front of its parent star  
37 as viewed by an observer) nearly twelve thousand stars of magnitude 11-16  
38 were observed simultaneously with a cadence of 512 or 32 seconds (i.e., a  
39 measurement every 512 or 32 seconds). For seismology about 10 stars with  
40 magnitude between 6 and 9 were monitored simultaneously during each run  
41 at a cadence of 32 seconds. After the initial observing run of nearly 60 days  
42 there were long runs of 150 days alternated with short runs of 20-30 days

---

<sup>1</sup>The CoRoT space mission was developed and operated by the CNES, with participa-  
tion of the Science Programs of ESA, ESA's RSSD, Austria, Belgium, Brazil, Germany,  
and Spain.

<sup>2</sup>*Kepler* is a NASA discovery class mission, whose funding is provided by NASA's  
Science Mission Directorate.

43 each monitoring a different patch of the sky around the so-called CoRoT  
44 eyes. See Baglin et al. (2006), Auvergne et al. (2009) for further technical  
45 details of the CoRoT telescope.

46 CoRoT has observed pre-main-sequence stars (e.g. Zwintz et al., 2013),  
47 stars on the main-sequence ranging from O and B type stars (e.g. Belka-  
48 cem et al., 2009; Degroote et al., 2010) to stars slightly more massive than  
49 the Sun (e.g. Michel et al., 2008), as well as more evolved subgiants (e.g.  
50 Deheuvels and Michel, 2011), red giants (e.g. De Ridder et al., 2009), and  
51 supergiants (Aerts et al., 2010b). Additionally, detailed studies of stars har-  
52 bouring planets have been performed (e.g. Ballot et al., 2011; Gaulme et al.,  
53 2010).

54 Launched in December 2006 the CoRoT mission had a nominal lifetime  
55 of 2.5 years. It exceeded this nominal period and has taken scientific data  
56 till November 2012.

## 57 1.2. *Kepler*

58 The *Kepler* mission was designed primarily to detect earth-size planets in  
59 or near the habitable zone (region around a star in which it is theoretically  
60 possible for a planet with sufficient atmospheric pressure to maintain liquid  
61 water on its surface) and to determine what percentage of the billions of stars  
62 in our galaxy have such planets. To this end a 0.95-meter Schmidt telescope  
63 was designed to be able to observe a 105 square-degree field of view. *Kepler*  
64 has been launched in 2009 and monitored about 150 000 stars at the same  
65 time in a single field (Cygnus-Lyra region) with magnitudes between 9 and  
66 16 and a cadence of 29.4 minutes (so-called long-cadence mode). Stars with  
67 oscillation periods longer than about an hour, such as A and F stars (e.g.  
68 Uytterhoeven et al., 2011), and B stars (e.g. Balona et al., 2011b) on the  
69 main sequence, red giants (e.g. Bedding et al., 2010), RR Lyrae stars (e.g.  
70 Kolenberg et al., 2010) as well as eclipsing binaries (e.g. Prša et al., 2011)  
71 could be observed in this way.

72 Additionally, the *Kepler* satellite was operated in a short cadence mode  
73 in which 512 stars could be observed simultaneously at a cadence of 58.85  
74 seconds (Gilliland et al., 2010). This allowed for asteroseismic analyses of  
75 Sun-like stars and subgiants (e.g. Chaplin et al., 2010) which show oscilla-  
76 tions with periods of the order of a few minutes. Other stars observed in  
77 this observing mode are compact oscillators such as sub-dwarf B stars (e.g.  
78 Kawaler et al., 2010) and white dwarfs (e.g. Córscico et al., 2012), as well as  
79 Ap stars (e.g. Balona et al., 2011a).

80 The nominal life time of the mission was 3.5 years. Following the nomi-  
81 nal lifetime, the scientific exploitation of *Kepler* was extended but a failure  
82 in a reaction wheel put the satellite in safe mode in May 2013. Since then  
83 scientific data acquisition has ceased. The *Kepler* team is exploring all possi-  
84 bilities to solve the problem and put *Kepler* back in scientific operation mode.

85  
86 The data of the CoRoT and *Kepler* satellites have already led to several  
87 breakthrough results in our understanding of the internal structures of stars  
88 as well as in the vast numbers and diversity of detected planetary systems.  
89 In the next section a more detailed description of asteroseismology is pre-  
90 sented followed by a selection of important asteroseismic results obtained  
91 with CoRoT and *Kepler* for low-mass main-sequence stars, subgiants, and  
92 red-giant stars. This review finishes with some future perspectives.

## 93 **2. Asteroseismology**

### 94 *2.1. Introduction*

95 Asteroseismology is the study of the internal structures of stars by means  
96 of their intrinsic global oscillations. The characteristics of these oscillations  
97 are determined by the stellar interior and hence it is possible to infer the  
98 stellar structure from the oscillations. Many (but, as far as we know, not all)  
99 stars across the Hertzsprung-Russell diagram oscillate.

100 Stellar oscillations can be characterised by their frequencies, typical life-  
101 time (coherence time), amplitudes and mode identification. Oscillation modes  
102 are identified by the radial order ( $n$ ) indicating the number of nodes in the  
103 radial direction, the spherical degree ( $\ell$ ) indicating the number of nodal lines  
104 on the surface, and the azimuthal order ( $m$ ) indicating the number of nodal  
105 lines that pass through the rotation axis. Examples of  $\ell = 3$  modi with dif-  
106 ferent  $m$  values are shown in Figure 1. The mode identification in terms of  
107  $n, \ell, m$ , the frequency and amplitude of the modes as well as effective tem-  
108 perature, surface gravity, and metallicity, allow for a study of the internal  
109 structure of the star. The internal stellar structure can be studied by com-  
110 paring the observational results with results from stellar models, or directly  
111 from the observational data as is the case for glitches (see Section 2.3.4). An  
112 example of model dependent results is presented by Metcalfe et al. (2012),  
113 while Mazumdar et al. (2012b) show model independent results.

114 There exist mainly two types of oscillators depending on the driving mech-  
115 anism and their resulting mode pattern.

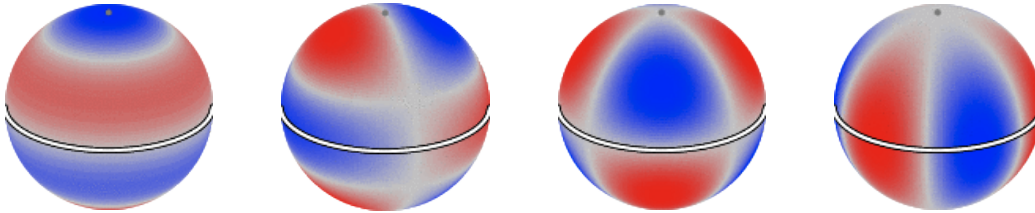


Figure 1: Schematic representation of  $\ell = 3$  oscillation modes with  $m = 0, 1, 2, 3$  from left to right. The blue areas indicate regions where the star expands while the red parts contract. The gray lines are the nodal lines with the dark gray dot at the top indicating the rotation axis, which lies in the plane of the paper. The equator is indicated in white. Figure obtained from non radial pulsator (NRP) animation creator (Schrijvers et al., 1997).

116 *2.2. Driving mechanisms*

117 *2.2.1. Heat engine*

118 Oscillations can be driven by a so-called heat engine. In this mechanism  
 119 a particular layer in the star gains heat during the compression part of the  
 120 oscillation cycle. This usually occurs in partially ionized layers of elements  
 121 with high opacity, such as hydrogen, helium, or iron. Inside these partially  
 122 ionized layers the energy, which would normally heat the zone, mostly goes  
 123 into increasing the ionization as the star is compressed. This increases the  
 124 opacity of the zone, trapping radiation more efficiently, and resulting in out-  
 125 ward pressure. The zone is then driven outwards, cooling as it rises, which  
 126 increases the opacity and outward pressure. Further cooling of the zone  
 127 results in recombination of the ionized material, and with that a sudden de-  
 128 crease in the opacity decreasing the outward pressure. Hence, the zone drops  
 129 back and the cycle can start again. Due to the role of opacity this is also  
 130 called  $\kappa$  mechanism.

131 The location of the layer(s) that act(s) as a heat engine is crucially im-  
 132 portant to effectively drive global oscillations as all other layers that lose  
 133 heat on compression damp the oscillations. See for more details Aerts et al.  
 134 (2010a).

135 Oscillators driven by the heat engine, such as Cepheids, have coherent  
 136 oscillation modes with very long lifetimes and hence their oscillation peaks  
 137 in the Fourier spectrum resemble  $\delta$ -functions. The observed oscillations are  
 138 affected by selection effects and the mode identification has to be obtained  
 139 from multi-colour photometry (amplitude ratios and / or phase differences),  
 140 or from high-resolution spectroscopy (line-profile variations).

141 *2.2.2. Stochastic driving*

142 Oscillations can be stochastically excited by the turbulent convection of  
143 stars (e.g. Goldreich and Keeley, 1977; Goldreich and Kumar, 1988). Ef-  
144 fectively, some of the convective energy is transferred into energy of global  
145 oscillations. The oscillations in the Sun are stochastically driven and damped.  
146 Hence these type of oscillations are referred to as solar-like oscillations. It  
147 is expected that in all stars with turbulent outer layers such oscillations are  
148 excited. For a recent extensive overview of solar-like oscillators see Chaplin  
149 and Miglio (2013). In addition to the oscillations the convection also pro-  
150 duces a convective background on which the p-mode spectrum is seated. See  
151 Mathur et al. (2011b) for a description and characterization of the convective  
152 background.

153 The stochastic driving and damping of solar-like oscillations results in a  
154 finite mode lifetime (few minutes to about hundred days) of the oscillation  
155 modes. This finite mode lifetime is visible as a typical width in the peaks  
156 representing the oscillations in the Fourier spectrum, with shorter lifetimes  
157 resulting in wider peaks. Additionally, in stochastic oscillators essentially all  
158 modes are excited albeit with different amplitudes. This results in a clear  
159 pattern of overtones in the Fourier spectrum (see top panel of Figure 2). This  
160 is of great value for identifying the oscillation modes.

161

162 For the remainder of this review only stars with stochastically-driven solar-  
163 like oscillations will be considered.

164 *2.3. Solar-like oscillators*

165 Stars with a convective zone that excite stochastic oscillations extend  
166 from low-mass ( $M \lesssim 2M_{\odot}$ ) main-sequence stars till evolved red giants. Stars  
167 on the main sequence are those that fuse hydrogen in their core. Then when  
168 the core hydrogen is exhausted, the stars start to burn hydrogen in a shell  
169 around an inert helium core, while the surface is cooling (subgiants). On the  
170 red-giant branch the luminosity and radii of the stars increase up to the onset  
171 of helium-core burning. Then the radii and surface temperatures decrease  
172 and the helium-core burning stars settle on the horizontal branch (also called  
173 red clump).

174 Oscillations can be trapped in a cavity in the outer layers of the star  
175 where the restoring force is pressure and the oscillations have the nature of  
176 standing acoustic waves. These oscillation modes are referred to as p-mode  
177 oscillations. The oscillations can also be trapped in an inner cavity in the

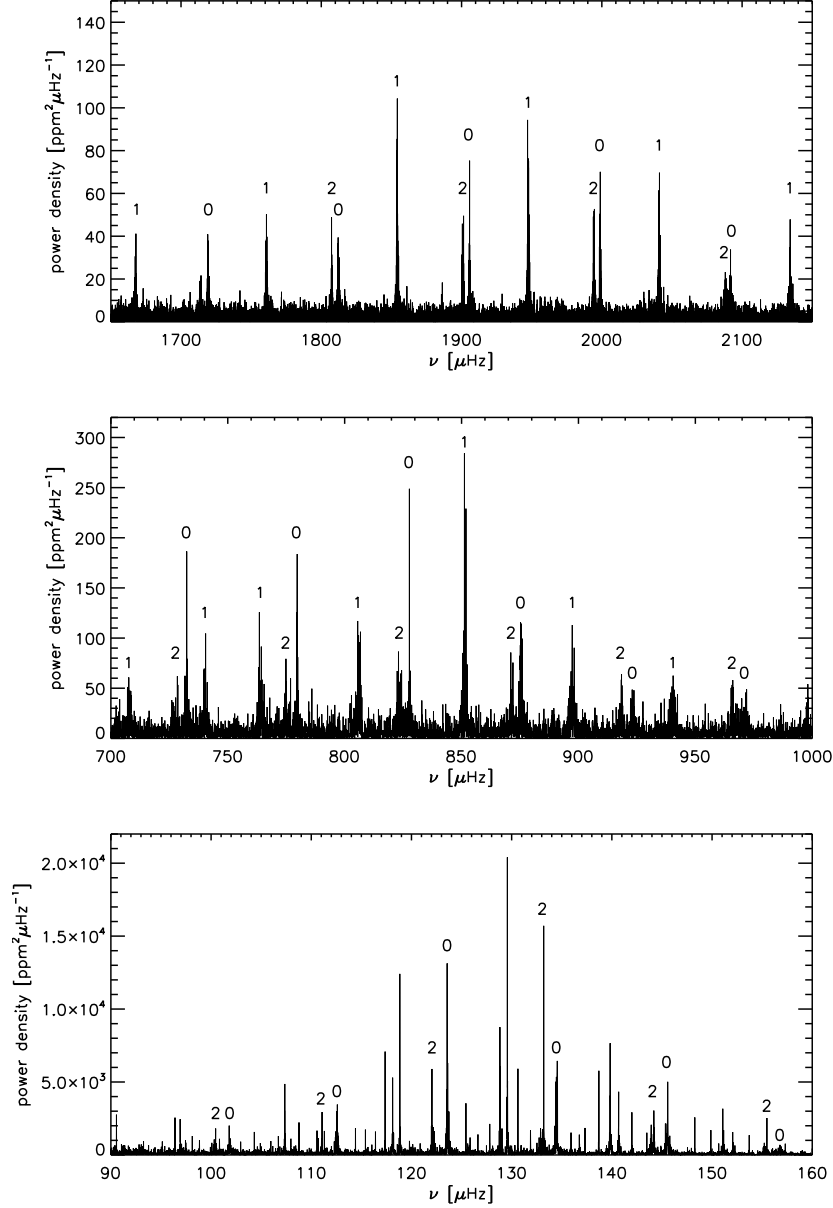


Figure 2: Fourier power density spectra of a main-sequence star (KIC 3656479 (top), Mathur et al., 2012), a subgiant (KIC 11395018 (middle), Mathur et al., 2011a), and a red giant (KIC 9145955, bottom). The numbers indicate the degree ( $\ell$ ) of the modes. The subgiant in the middle panel has a mixed mode pair at 740.3 and 764.0  $\mu\text{Hz}$ . This can be identified by the fact that two  $\ell = 1$  modes are present between the  $\ell = 0, 2$  pairs at  $\sim 730$  and  $770$   $\mu\text{Hz}$ . The vertical dotted lines indicate  $\nu_{\text{max}}$  (Eq. 1) and the horizontal dashed-dotted line (top panel) indicates  $\Delta\nu$  (Eq. 3).

178 inner radiative region of the stars where the restoring force is buoyancy and  
 179 the oscillations have the character of standing gravity waves. These are called  
 180 g-mode oscillations.

181 In the Sun the lower turning points of low-degree non-radial modes –that  
 182 can be observed in other stars– are roughly between 0.05 and 0.2 solar radius,  
 183 depending on the frequency and degree of the mode (e.g. Lopes and Turck-  
 184 Chieze, 1994; García et al., 2008). Note, however, that the non-radial p modes  
 185 are most sensitive to the part of the cavity where they spend most time, i.e.,  
 186 the part where the sound speed is lowest. The sound speed decreases towards  
 187 the surface, and hence the oscillations carry most information of the outer  
 188 part of the cavity. The g modes are most sensitive in a radiative region  
 189 deeper in the star below the lower turning point of the p modes. The dipole  
 190 asymptotic g-mode spacing in the Sun was measured by García et al. (2007).  
 191 Unfortunately, due to the small amplitude of the g modes at the surface of the  
 192 Sun, it has not been possible to detect g modes directly. When stars evolve  
 193 to the subgiant phase the frequencies of the oscillations in the p- and g-mode  
 194 cavities nearly overlap and a few so-called mixed modes can be observed (see  
 195 middle panel of Figure 2). Such modes have g-mode nature in the radiative  
 196 interior and p-mode nature in the outer cavity. For further evolved red-giant  
 197 stars a large number of frequencies in the g-mode cavity overlap with the  
 198 oscillation frequencies in the p-mode cavity and many mixed modes can be  
 199 observed (see bottom panel of Figure 2).

### 200 2.3.1. Pressure modes

201 P-mode oscillations in the Sun have a typical period of about 5 minutes  
 202 which corresponds to frequencies of roughly 3 mHz. Lower-mass stars on the  
 203 main-sequence are smaller and have oscillations with shorter periods, i.e.,  
 204 higher frequencies. More evolved stars with larger radii show oscillations  
 205 with longer periods of hours to days, resulting in frequencies in the sub-mHz  
 206 or  $\mu\text{Hz}$  regime. The typical frequency region in which the acoustic modes  
 207 oscillate can be characterised by  $\nu_{\text{max}}$ , the frequency of maximum oscillation  
 208 power (vertical dotted lines in Fig. 2). This is an important diagnostic as it  
 209 scales with the mass ( $M$ ), radius ( $R$ ), and effective temperature ( $T_{\text{eff}}$ ) of the  
 210 star (e.g. Brown et al., 1991; Kjeldsen and Bedding, 1995; Belkacem et al.,  
 211 2011):

$$\nu_{\text{max}} \propto \frac{M}{R^2 \sqrt{T_{\text{eff}}}} \propto \frac{g}{\sqrt{T_{\text{eff}}}}, \quad (1)$$

212 with  $g$  the surface gravity.

213 The pattern of the frequencies in the Fourier spectrum can be described  
 214 asymptotically by (Tassoul, 1980; Gough, 1986):

$$\nu_{n,\ell} \simeq \Delta\nu\left(n + \frac{\ell}{2} + \epsilon\right) - \delta\nu_{n,\ell}, \quad (2)$$

215 where  $\nu$  is frequency and  $\epsilon$  is a phase term.  $\Delta\nu$  is the regular spacing in  
 216 frequency of oscillations with the same degree  $\ell$  and consecutive orders  $n$   
 217 (horizontal dashed-dotted line in the top panel of Fig. 2). This is proportional  
 218 to the inverse of the acoustic diameter, i.e. the sound travel time across a  
 219 stellar diameter. Furthermore, it can be shown that  $\Delta\nu$  is proportional to  
 220 the square root of the mean density ( $\bar{\rho}$ ) of the star (Ulrich, 1986):

$$\Delta\nu = \nu_{n,\ell} - \nu_{n-1,\ell} = \left(2 \int \frac{dr}{c}\right)^{-1} \propto \sqrt{\bar{\rho}}, \quad (3)$$

221 with  $c$  the adiabatic sound speed and  $r$  the distance to the centre of the star.  
 222 Note that slightly different methods to measure  $\nu_{\max}$  and  $\Delta\nu$  are available  
 223 (e.g. Huber et al., 2009; Mosser and Appourchaux, 2009; Hekker et al., 2010;  
 224 Kallinger et al., 2010; Mathur et al., 2010). It has been shown that the differ-  
 225 ent determinations are consistent within their uncertainties and definitions  
 226 (e.g. Verner et al., 2011; Hekker et al., 2011, 2012).

227 Finally,  $\delta\nu_{n,\ell}$  is the so-called small frequency separation which can be  
 228 approximated asymptotically by (e.g. Gough, 1986):

$$\delta\nu_{n,\ell} = \nu_{n,\ell} - \nu_{n-1,\ell+2} \simeq -(4\ell + 6) \frac{\Delta\nu}{4\pi^2\nu_{n,\ell}} \int_0^R \frac{dc}{dr} \frac{dr}{r}. \quad (4)$$

229 For main-sequence stars Eq. 4 is rather strongly weighted towards the central  
 230 parts of the star. Hence  $\delta\nu_{n,\ell}$  provides a measure of the helium content in  
 231 the core. In the core of more evolved stars the increase in the helium content  
 232 causes a reduction in the sound speed, and hence a reduced weight of the  
 233 central parts of the star in the integral of Eq. 4. Therefore in more evolved  
 234 stars  $\delta\nu_{n,\ell}$  does not provide a measure of the helium content in the core.

235 The near-surface regions of stars are difficult to model properly due to  
 236 convection. Additionally the oscillations are strongly non-adiabatic in the  
 237 superficial layers. These near-surface problems cause a shift in the frequencies  
 238 of stellar models compared to the observed frequencies, which should be  
 239 accounted for. The large and small frequency separation (Eqs. 3 and 4) are  
 240 also affected by the near-surface problems although less severely. To eliminate

241 the influence of the near-surface region, frequency ratios such as  $r_{02}$  (Eq. 5)  
 242 can be constructed, which are essentially independent of the near-surface  
 243 problems (e.g. Roxburgh and Vorontsov, 2003; Roxburgh, 2005).

$$r_{02} = \frac{\nu_{n,0} - \nu_{n-1,2}}{\nu_{n,1} - \nu_{n-1,1}} \quad (5)$$

### 244 2.3.2. Gravity modes

245 The g modes in the inner radiative region have a high number of radial  
 246 nodes ( $n_g$ ) due to the high density of the core. These oscillation modes follow  
 247 an asymptotic approximation equivalent to the p modes, but with a regular  
 248 spacing in period ( $\Delta\Pi$ ):

$$\Delta\Pi_\ell = \frac{2\pi^2}{\sqrt{\ell(\ell+1)}} \left( \int \frac{N}{r} dr \right)^{-1} \quad (6)$$

249 with  $N$  the so-called buoyancy frequency, i.e., the characteristic frequency  
 250 for internal gravity waves (e.g. Tassoul, 1980).

### 251 2.3.3. Mixed modes

252 In subgiants and red giants the frequencies in both the p-mode cavity in  
 253 the outer atmosphere and the g-mode cavity in the inner radiative region  
 254 have similar values and a coupling between the cavities can persist. In that  
 255 case a p and g mode with similar frequencies and same spherical degree  
 256 undergo a so-called avoided crossing. The interactions between the modes  
 257 will affect (or bump) the frequencies. This bumping can be described as a  
 258 resonance interaction of two oscillators (e.g. Aizenman et al., 1977; Deheuvels  
 259 and Michel, 2010; Benomar et al., 2013). This causes additional non-radial  
 260 ( $\ell > 0$ ) mixed modes with dual p-g character to appear in the near regular  
 261 p-mode frequency pattern described above (see middle and bottom panel of  
 262 Figure 2). These mixed modes show a predictable pattern in period spacing  
 263 originating from the g-mode nature and the bumping with the p modes.

### 264 2.3.4. Sharp changes in stellar properties: Glitches

265 Information on specific transition regions in a star, such as the boundaries  
 266 of convective zones or ionization zones of helium or hydrogen, can be obtained  
 267 from the fact that, at such boundaries, the properties of the star change on a  
 268 scale substantially smaller than the local wavelength of the oscillations (e.g.  
 269 Vorontsov, 1988; Gough, 1990). These sharp features (also called glitches)

270 cause oscillatory variations in the frequencies with respect to the pattern  
271 described in Eq. 2, where the period of the variation depends on the location  
272 of the feature, while its amplitude depends on the detailed properties of the  
273 feature. Note that the determination of glitches is completely independent  
274 of stellar models.

### 275 *2.3.5. Rotation*

276 Stellar rotation lifts the degeneracy of non-radial modes, producing a mul-  
277 tiplet of  $(2\ell + 1)$  frequency peaks in the Fourier spectrum for each mode. The  
278 frequency separation between two mode components of a multiplet is related  
279 to the angular velocity of the stellar material in the propagation region, under  
280 the assumption of the absence of magnetic splitting. This allows us to derive  
281 the rotation rate of the star in the region to which the mode is most sensi-  
282 tive. The relative height of the mode components in a multiplet is sensitive  
283 to the inclination angle at which the star is viewed (Gizon and Solanki, 2003).  
284

285 Note that there are several excellent review papers by Christensen-Dalsgaard  
286 (e.g. Christensen-Dalsgaard, 2004, 2011, 2012) which provide a thorough the-  
287 oretical overview of solar-like oscillations.

## 288 **3. Recent results from CoRoT and *Kepler***

289 In this section a selection of the results obtained with CoRoT and *Kepler*  
290 for main-sequence stars and red-giant stars is presented.

### 291 *3.1. Main-sequence stars*

#### 292 *3.1.1. F-stars*

293 Early results from CoRoT came from a number of preselected main-  
294 sequence stars that are slightly hotter than the Sun (Michel et al., 2008)  
295 of which HD49933 became the best known ‘prototype’. This star is an F5V  
296 star about 1000 K hotter than the Sun. In these hotter stars the stochastic  
297 oscillations have shorter lifetimes, which results in wide peaks in the Fourier  
298 spectrum. Due to this effect the  $\ell = 2$  and  $\ell = 0$  modes might overlap in  
299 their frequency values. This causes difficulties for the mode identification  
300 (e.g. Appourchaux et al., 2008; Benomar et al., 2010). This phenomenon is  
301 also seen in other F stars observed with CoRoT (e.g. Barban et al., 2009;  
302 García et al., 2009) and *Kepler* (e.g. Appourchaux et al., 2012a,b) as well as  
303 for oscillations in F-stars observed with radial velocity measurements such

304 as Procyon (Hekker et al., 2008; Arentoft et al., 2008; Bedding et al., 2010;  
305 Huber et al., 2011). White et al. (2012) have now devised a method based on  
306 the phase term  $\epsilon$  (see Eq. 2), which seems to be able to identify the correct  
307 scenario.

### 308 *3.1.2. Planet-hosting stars*

309 The power of asteroseismology for planet-hosting stars lies in the determi-  
310 nation of accurate stellar parameters. From the detection of exoplanets using  
311 the transit method as done by CoRoT and *Kepler* it is possible to obtain the  
312 planetary properties as a function of the host-star properties. Hence, the ac-  
313 curacy of, for instance, the determined planetary radius depends crucially on  
314 the stellar radius. Stellar radii from asteroseismology have typical uncertain-  
315 ties of the order of 2-3% and are thus far better than can be obtained from  
316 the position in the H-R diagram, which is often the alternative. Such accu-  
317 rate stellar properties have led to breakthrough results, such as CoRoT-7b,  
318 the first transiting super-earth (e.g. Léger et al., 2009; Wagner et al., 2012,  
319 and references therein); Kepler-21b, a 1.6 earth-radius planet (Howell et al.,  
320 2012); Kepler-36, a system with a pair of planets with neighbouring orbits  
321 and dissimilar densities (Carter et al., 2012); or Kepler-37b, a sub-Mercury  
322 sized planet (Barclay et al., 2013).

323 From asteroseismology it is also possible to obtain the stellar rotation  
324 and the inclination angle, i.e., the angle between the rotation axis and the  
325 observer (e.g. Ballot et al., 2011). These parameters can be used to study  
326 the obliquity of exoplanet host stars, i.e., the angle between the stellar spin  
327 axis and the planetary orbital axis. Chaplin et al. (2013) present such a  
328 study for two planetary systems and find that coplanar orbits are favored  
329 in both systems, and that the orientations of the planetary orbits and the  
330 stellar rotation axis are correlated. Huber et al. (2013) revisited all *Kepler*  
331 planet-host stars showing pulsations and refined the fundamental properties  
332 of these planet-candidate host stars.

## 333 *3.2. Evolved stars*

### 334 *3.2.1. Non-radial oscillations*

335 Before the first results of CoRoT it was debated whether non-radial oscil-  
336 lations would be observable for red-giant stars. It was thought that non-radial  
337 oscillations would be damped in the inner g-mode cavity. This was based on  
338 the analysis of WIRE data of the K0III star  $\alpha$  UMa (Buzasi et al., 2000)  
339 and the subsequent theoretical interpretation (Dziembowski et al., 2001).

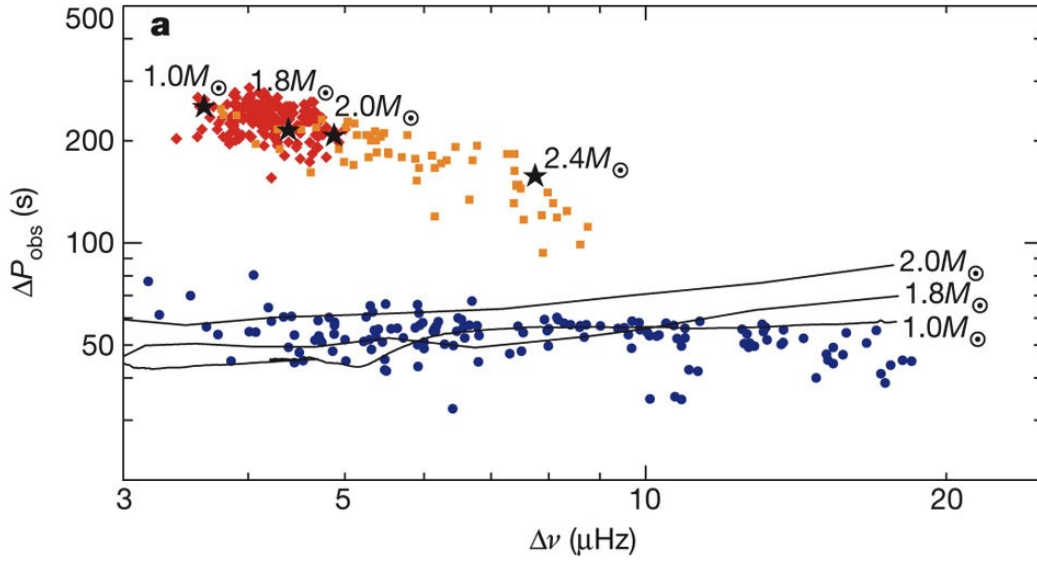


Figure 3: Observed period spacing ( $\Delta P$ ) as a function of large frequency separation ( $\Delta \nu$ ) with stars in the hydrogen-shell-burning phase on the red-giant branch shown in blue dots and the stars in the helium-core-burning phase shown in red diamonds and orange squares. The solid lines show average observable period spacings for ASTEC (Christensen-Dalsgaard, 2008) models of hydrogen-shell-burning giants on the red-giant branch as they evolve from right to left. The black stars show theoretical period spacings calculated in the same way, for four models of helium-core-burning stars that are midway through that phase (core-helium fraction 50%). The  $2.4 M_{\odot}$  model was calculated with ASTEC and commenced helium-burning without passing through a helium flash. The other three models, which did undergo a helium flash, were computed using the ATON code (Ventura et al., 2008). Solar metallicity was adopted for all models, which were computed without mass loss. Figure adapted from Bedding et al. (2011).

340 Observations in a radial velocity multi-site campaign of two other stars,  $\xi$   
 341 Hydrae and  $\epsilon$  Ophiuchi, were interpreted accordingly (Frandsen et al., 2002;  
 342 Stello et al., 2006; De Ridder et al., 2006; Mazumdar et al., 2009). However,  
 343 investigation of spectral-line shapes of these stars revealed that non-radial  
 344 oscillations are detectable in red-giant stars (Hekker et al., 2006). Data from  
 345 the CoRoT mission confirmed this unambiguously (De Ridder et al., 2009)  
 346 with hundreds of stars showing a Fourier spectrum with a similar pattern  
 347 of  $\ell = 0, 1, 2$  modes as present in the Sun. At the same time this was also  
 348 understood from theoretical calculations by Dupret et al. (2009). Not only  
 349 did these authors predict that non-radial oscillations with predominantly p-  
 350 mode nature could reach observable heights in the Fourier spectrum, they  
 351 also predicted the presence of additional g-dominated mixed modes.

352 Gravity-dominated mixed modes in red-giant stars have recently been  
 353 discovered observationally for  $\ell = 1$  modes by Beck et al. (2011). From these  
 354 mixed modes the period spacings (see Eq. 6) can be derived. Bedding et al.  
 355 (2011) and Mosser et al. (2011a) showed that the observed period spacings  
 356 of red giants in the hydrogen-shell-burning phase ascending the red-giant  
 357 branch is significantly different from the period spacing for red giants also  
 358 burning helium in the core. This provides a clear separation into these two  
 359 groups of stars that are superficially very similar (see Figure 3). This effect  
 360 was explained by Christensen-Dalsgaard (2011) as being due to convection  
 361 in the central regions of the core in the helium-burning stars. The buoyancy  
 362 frequency ( $N$ ) is nearly zero in the convective region. As the period spacing  
 363 is inversely proportional to the integral over  $N$  (see Eq. 6), this increases the  
 364 period spacing compared to a star without a convective region in the core.

### 365 3.2.2. Rotation

366 Mixed modes are most sensitive in either the internal or the outer region  
 367 of the star depending on their predominant g- or p-mode nature. Hence the  
 368 characteristics of these modes with different nature can reveal information  
 369 on properties at different depths in the star. One of these characteristics is  
 370 the splitting of the mode in  $m = -\ell, \dots, \ell$  azimuthal orders due to rotation.  
 371 The rotational splitting of dipole mixed modes with different p-g nature  
 372 have been measured (Beck et al., 2012) and show that for a red-giant branch  
 373 star the core rotates approximately ten times faster than the surface (see  
 374 Figure 4). This discovery was followed by a result for a low-luminosity red-  
 375 giant branch star for which the core rotation is about five times faster than  
 376 the surface rotation (Deheuvels et al., 2012). Subsequently, Mosser et al.

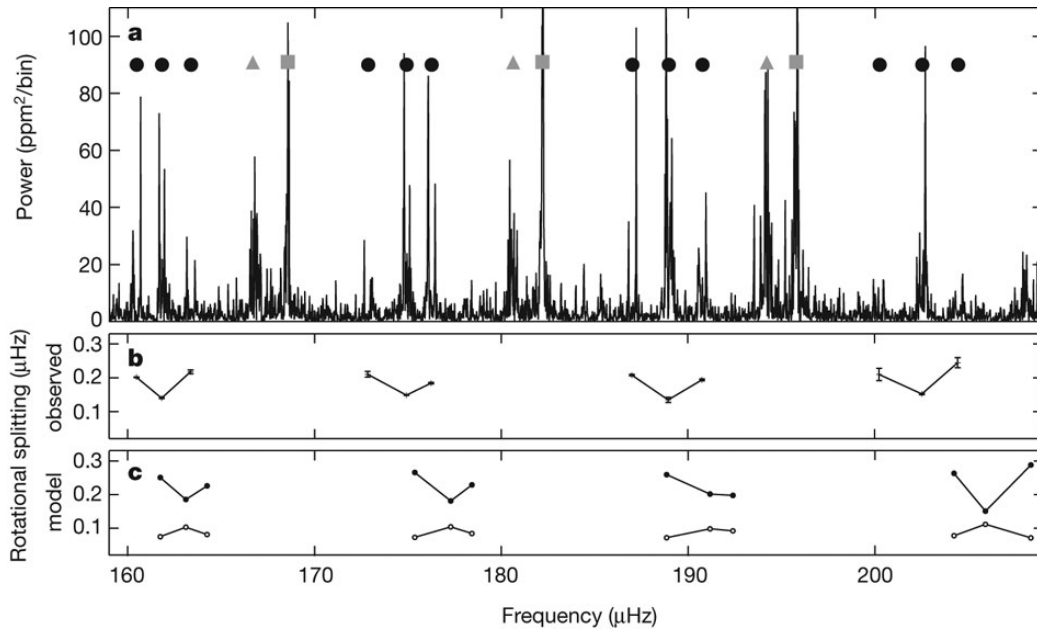


Figure 4: Top: Fourier spectrum of a rotating red giant. Grey squares indicate radial modes, grey triangles indicate  $\ell = 2$  modes, and black circles indicate  $\ell = 1$  rotational multiplets. Middle: the observed rotational splitting for individual  $\ell = 1$  modes. Bottom: theoretically predicted rotational splitting assuming two different rotation laws. Dots: splitting for non-rigid rotation for the case of a core rotation ten times faster than the surface rotation, which resembles the observations qualitatively well. Open circles: theoretical splittings for rigid rotation, which show a trend opposite to the observed one, with the largest splitting in the centre of the dipole forest and lower splitting in gravity-dominated modes. Figure taken from Beck et al. (2012).

377 (2012) showed that stars ascending the red-giant branch experience a small  
 378 increase of the core rotation followed by a significant slow-down in the later  
 379 stages of the red-giant branch resulting in slower rotating cores in red-clump  
 380 (or horizontal-branch) stars compared to stars on the red-giant branch.

### 381 3.3. Glitches

382 Only with the data from CoRoT and *Kepler* it has become possible to  
 383 measure glitches, i.e., the signature of sharp internal structure changes, in  
 384 other stars than the Sun. Miglio et al. (2010) studied the internal structure  
 385 of the CoRoT target HR 7349 from frequencies obtained by Carrier et al.  
 386 (2010). Miglio et al. (2010) interpreted a periodic component in the oscil-  
 387 lation frequencies as caused by a local depression of the sound speed that

388 occurs in the helium second-ionization region at a relative acoustic radius  
389 of  $\sim 0.55$  (in the Sun the helium second-ionization region lies at a relative  
390 acoustic radius of  $\sim 0.83$  and the base of the convection zone at a relative  
391 acoustic radius of  $\sim 0.4$ ). Subsequently, Mazumdar et al. (2012a) studied the  
392 sharp internal structure changes of HD49933 and were able to find both the  
393 signatures of the helium second-ionization zone and of the base of the con-  
394 vective envelope. Similar studies of 19 stars observed with *Kepler* found that  
395 the extracted locations of the layers of sharp variation in sound speed are  
396 consistent with representative models of these stars (e.g. Mazumdar et al.,  
397 2012b).

### 398 3.4. Ensemble asteroseismology

399 Before the CoRoT and *Kepler* era solar-like oscillations were confirmed  
400 in 10-20 stars. This number increased significantly with CoRoT and *Kepler*  
401 data. For example, with CoRoT the number of red giants with detected  
402 solar-like oscillations increased from three to hundreds. These large numbers  
403 allowed for the first time to investigate an ensemble of stars as a whole, i.e.,  
404 to perform statistical studies of intrinsic stellar properties (such as mass and  
405 radius) and to test theories of stellar evolution. Such “ensemble asteroseis-  
406 mology” studies were performed by e.g. Hekker et al. (2009); Huber et al.  
407 (2010); Kallinger et al. (2010); Mosser et al. (2010). These studies led, among  
408 others, to observational evidence for a tight correlation between  $\nu_{\max}$  and  $\Delta\nu$   
409 (Hekker et al., 2009; Stello et al., 2009; Mosser et al., 2010). Additionally, it  
410 was found that oscillations in red giants follow a universal pattern (Mosser  
411 et al., 2011b). Furthermore, investigations of properties, such as the am-  
412 plitudes of the oscillations, as a function of evolution have been presented  
413 (Huber et al., 2010). Miglio et al. (2009) followed this up with a comparison  
414 of the observed distribution of the large frequency separation with distribu-  
415 tions from different synthetic populations showing that it is not likely that a  
416 recent starburst has taken place in our part of the Milky Way.

417 With *Kepler* the number of stars with detected solar-like oscillations  
418 has been increased to tens of thousands, among which about 500 are main-  
419 sequence and subgiant stars. An ensemble study of these main-sequence and  
420 subgiant stars was performed by Chaplin et al. (2011). One of the main con-  
421 clusions resulting from this work concerned the similarity in the observed and  
422 simulated radius distributions as well as the difference between the stellar-  
423 mass distribution derived observationally from the asteroseismic measure-  
424 ments and the mass distribution of synthetic populations (see also Figure 5).

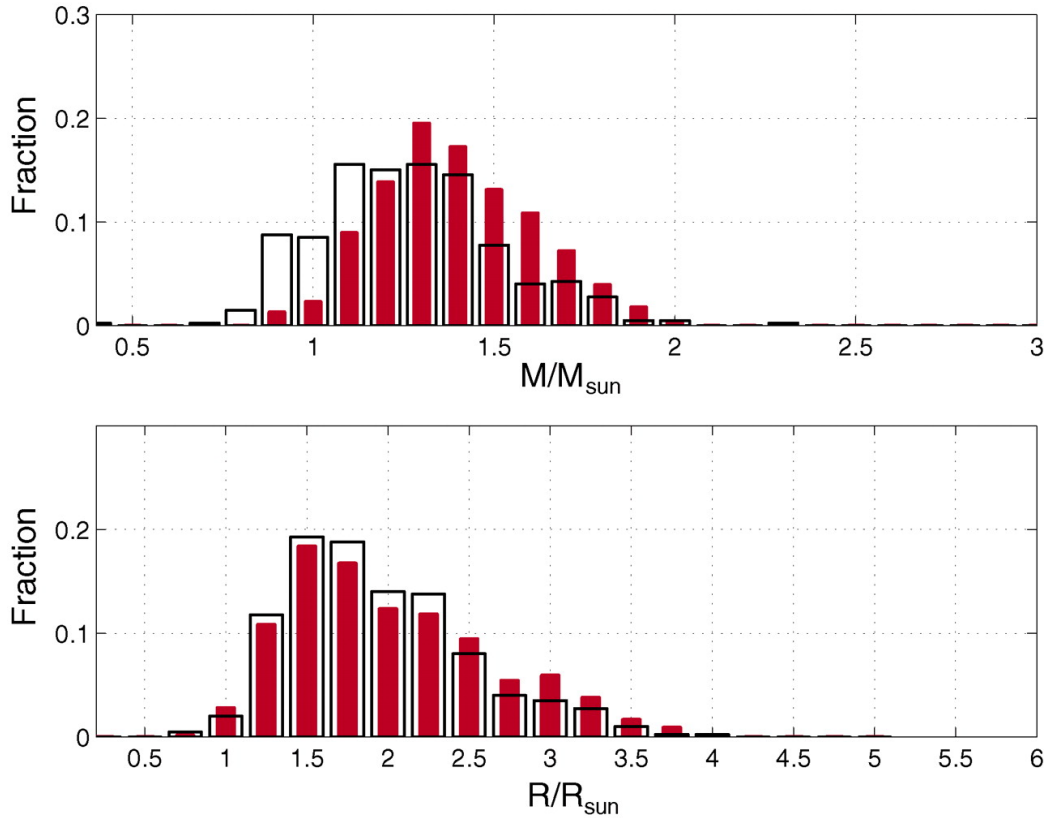


Figure 5: Black lines show histograms of the observed distribution of masses (top) and radii (bottom) of the *Kepler* main-sequence and subgiants ensemble (Chaplin et al., 2011). In red, the predicted distributions from population-synthesis modeling, after correction for the effects of detection bias. The population modeling was performed by using the TRILEGAL code (Girardi et al., 2005; Miglio et al., 2009). Figure taken from Chaplin et al. (2011).

425 On the assumption that the observed masses and radii are robust, this result  
426 may have implications for both the currently expected star-formation rate  
427 as well as initial-mass function of stars. Mixing or overshooting of material  
428 between different layers (including stellar cores) and the choice of the so-  
429 called mixing-length parameter, which measures the typical length scale of  
430 the convection, may also be relevant (Chaplin et al., 2011).

431 A more detailed review of ensemble asteroseismology based on CoRoT  
432 and *Kepler* data has been presented by Chaplin and Miglio (2013).

#### 433 4. Future

434 CoRoT and *Kepler* have both exceeded their minimal lifetime, but are  
435 currently out of operation since November 2<sup>nd</sup> 2012 (CoRoT) and mid May  
436 2013 (*Kepler* in safe mode).

437 Notwithstanding the technical problems at these stages, both CoRoT  
438 and *Kepler* have done an outstanding job and provided the community with  
439 a wealth of data that revolutionised the fields of extra-solar planets and  
440 asteroseismology. Data from these satellites revealed, among others, the  
441 possibility to distinguish between red-giant branch stars and red-clump stars,  
442 to determine differential rotation between the core and the outer layers of the  
443 stars, as well as the location of sharp internal structure changes in stars other  
444 than the Sun. Nevertheless, there exist still open questions such as, what  
445 are the ages of stars, or how do the large variety of planetary systems form.  
446 To answer these questions dedicated efforts for several new instruments are  
447 underway:

- 448 • BRITE-Constellation (BRiGht Target Explorer) is a network of nano-  
449 satellites with different colour filters to investigate the properties of the  
450 brightest stars in the sky (Kaiser et al., 2012). The Austrian BRITE-  
451 satellites have been launched successfully on February 25, 2013.
- 452 • On April 5, 2013, NASA announced the selection of the Transiting Ex-  
453 oplanet Survey Satellite (TESS). TESS will perform an all-sky survey  
454 to discover transiting exoplanets ranging from Earth-sized to gas giants  
455 in orbit around the nearest and brightest stars in the sky. Its goal is to  
456 identify terrestrial planets in the habitable zones of nearby stars. This  
457 mission will also be very useful to obtain accurate asteroseismology for  
458 the nearest and brightest stars.

459 • PLATO (PLANetary Transits and Oscillations of stars) is a candidate  
460 mission for ESA. The primary goal of PLATO is to open a new way in  
461 exoplanetary science, by providing a full statistical analysis and char-  
462 acterisation of exoplanetary systems around stars that are bright and  
463 nearby enough to allow for simultaneous detailed studies of their host  
464 stars (Rauer, 2012).

465 • From the ground a network of telescopes is under construction. SONG  
466 (Stellar Observations Network Group) is a Danish-led project to con-  
467 struct a global network of 1m telescopes. These telescopes have a high-  
468 resolution spectrograph dedicated to asteroseismic measurements. The  
469 first telescope has been built at Observatorio del Teide, Tenerife, and  
470 will enter the operation mode in the summer of 2013 (Uytterhoeven  
471 et al., 2012). Another telescope of the SONG network is currently  
472 under development in China (Deng et al., 2013).

473 Spectroscopic observations of solar-like oscillations have the advantage  
474 that the granulation signal is less prominent and hence the oscilla-  
475 tions are more prominent. Furthermore, it is more likely to observe  
476  $\ell = 3$  modes using spectroscopic observations providing additional con-  
477 straints for the determination of the stellar structures.

478 All these efforts are complementary to CoRoT and *Kepler* in both ob-  
479 serving strategy and in the target stars. BRITe, TESS, and PLATO will aim  
480 at much brighter stars than CoRoT and *Kepler* which will allow for comple-  
481 mentary ground-based efforts to determine effective temperatures and metal-  
482 licities, which are important observables for stellar modeling. Furthermore,  
483 these missions will observe different parts of the sky allowing for stellar-  
484 population studies of different fields. TESS will even perform an all-sky  
485 survey albeit at the cost of shorter datasets, i.e., lower frequency resolution.  
486 PLATO will observe two different large fields ( $\sim 500$  square degrees) for  
487 about two to three years each before going to a step and stare mode. This  
488 will have the advantage of long datasets for tens of thousands of bright stars,  
489 which are currently lacking. Additionally, the synergy with Gaia (Torra and  
490 Gaia group, 2013) will allow for accurate distance and luminosity determi-  
491 nations. Finally, BRITe has different colour filters which will be of prime  
492 importance for the mode identification of oscillations driven by the heat-  
493 engine mechanism.

494 With the efforts that are currently underway future high-quality astero-

495 seismic observations are secured. These efforts are necessary to fully under-  
496 stand the internal structures of stars including their ages and planet forma-  
497 tion scenarios.

498

499 Finally, the CoRoT and *Kepler* legacy is a truly incredible amount of very  
500 high quality data. These data are of unprecedented quality in terms of signal-  
501 to noise ratio, continuity and total length of the timeseries as well as the vast  
502 number and range of different stars. The analysis and interpretation of these  
503 data will continue to reveal important results. These add to the wealth of  
504 results already obtained and (partly) described in this review, indicating the  
505 significant impact of asteroseismic results from CoRoT and *Kepler* on our  
506 understanding of stellar structure and evolution.

## 507 **5. Acknowledgements**

508 SH would like to thank Anwesh Mazumdar and Maarten Mooij for useful  
509 discussions and for providing detailed feedback on earlier drafts. SH also  
510 wants to thank the referee R.A. García for critical comments that improved  
511 the paper significantly. SH acknowledges financial support from the Nether-  
512 lands Organisation for Scientific Research (NWO).

## 513 **References**

514 Aerts, C., Christensen-Dalsgaard, J., Kurtz, D. W., 2010a. Asteroseismology.

515 Aerts, C., Lefever, K., Baglin, A., et al., Apr. 2010b. Periodic mass-loss  
516 episodes due to an oscillation mode with variable amplitude in the hot  
517 supergiant HD 50064. *A&A* 513, L11.

518 Aizenman, M., Smeyers, P., Weigert, A., Jun. 1977. Avoided Crossing of  
519 Modes of Non-radial Stellar Oscillations. *A&A* 58, 41.

520 Appourchaux, T., Benomar, O., Gruberbauer, M., et al., Jan. 2012a. Oscil-  
521 lation mode linewidths of main-sequence and subgiant stars observed by  
522 Kepler. *A&A* 537, A134.

523 Appourchaux, T., Chaplin, W. J., García, R. A., et al., Jul. 2012b. Oscilla-  
524 tion mode frequencies of 61 main-sequence and subgiant stars observed by  
525 Kepler. *A&A* 543, A54.

- 526 Appourchaux, T., Michel, E., Auvergne, M., et al., Sep. 2008. CoRoT sounds  
527 the stars: p-mode parameters of Sun-like oscillations on HD 49933. *A&A*  
528 488, 705–714.
- 529 Arentoft, T., Kjeldsen, H., Bedding, T., et al., Nov. 2008. A Multisite Cam-  
530 paign to Measure Solar-like Oscillations in Procyon. I. Observations, Data  
531 Reduction, and Slow Variations. *ApJ* 687, 1180–1190.
- 532 Auvergne, M., Bodin, P., Boisnard, L., et al., Oct. 2009. The CoRoT satellite  
533 in flight: description and performance. *A&A* 506, 411–424.
- 534 Baglin, A., Auvergne, M., Barge, P., et al., Nov. 2006. Scientific Objectives  
535 for a Minisat: CoRoT. In: Fridlund, M., Baglin, A., Lochard, J., Conroy,  
536 L. (Eds.), *ESA Special Publication*. Vol. 1306 of *ESA Special Publication*.  
537 p. 33.
- 538 Ballot, J., Gizon, L., Samadi, R., et al., Jun. 2011. Accurate p-mode mea-  
539 surements of the G0V metal-rich CoRoT target HD 52265. *A&A* 530, A97.
- 540 Balona, L. A., Cunha, M. S., Kurtz, D. W., et al., Jan. 2011a. Kepler obser-  
541 vations of rapidly oscillating Ap,  $\delta$  Scuti and  $\gamma$  Doradus pulsations in Ap  
542 stars. *MNRAS* 410, 517–524.
- 543 Balona, L. A., Pigulski, A., Cat, P. D., et al., Jun. 2011b. Kepler observations  
544 of the variability in B-type stars. *MNRAS* 413, 2403–2420.
- 545 Barban, C., Deheuvels, S., Baudin, F., et al., Oct. 2009. Solar-like oscillations  
546 in HD 181420: data analysis of 156 days of CoRoT data. *A&A* 506, 51–56.
- 547 Barclay, T., Rowe, J. F., Lissauer, J. J., et al., Feb. 2013. A sub-Mercury-  
548 sized exoplanet. *Nature* 494, 452–454.
- 549 Beck, P. G., Bedding, T. R., Mosser, B., et al., Apr. 2011. Kepler Detected  
550 Gravity-Mode Period Spacings in a Red Giant Star. *Science* 332, 205.
- 551 Beck, P. G., Montalban, J., Kallinger, T., et al., Jan. 2012. Fast core rotation  
552 in red-giant stars as revealed by gravity-dominated mixed modes. *Nature*  
553 481, 55–57.
- 554 Bedding, T. R., Huber, D., Stello, D., et al., Apr. 2010. Solar-like Oscillations  
555 in Low-luminosity Red Giants: First Results from Kepler. *ApJ* 713, L176–  
556 L181.

- 557 Bedding, T. R., Kjeldsen, H., Butler, R. P., McCarthy, C., Marcy, G. W.,  
558 O’Toole, S. J., Tinney, C. G., Wright, J. T., Oct. 2004. Oscillation Fre-  
559 quencies and Mode Lifetimes in  $\alpha$  Centauri A. *ApJ* 614, 380–385.
- 560 Bedding, T. R., Mosser, B., Huber, D., et al., Mar. 2011. Gravity modes as a  
561 way to distinguish between hydrogen- and helium-burning red giant stars.  
562 *Nature* 471, 608–611.
- 563 Belkacem, K., Goupil, M. J., Dupret, M. A., et al., Jun. 2011. The underlying  
564 physical meaning of the  $\nu_{max} - \nu_c$  relation. *A&A* 530, A142.
- 565 Belkacem, K., Samadi, R., Goupil, M.-J., et al., Jun. 2009. Solar-Like Oscil-  
566 lations in a Massive Star. *Science* 324, 1540.
- 567 Benomar, O., Baudin, F., Marques, J. P., et al., Dec. 2010. Spectrum analysis  
568 and seismic interpretation of a solar-like pulsator (HD 49933) observed by  
569 CoRoT. *Astronomische Nachrichten* 331, 956.
- 570 Benomar, O., Bedding, T. R., Mosser, B., et al., Apr. 2013. Properties of  
571 Oscillation Modes in Subgiant Stars Observed by Kepler. *ApJ* 767, 158.
- 572 Borucki, W., Koch, D., Basri, G., et al., May 2008. Finding Earth-size planets  
573 in the habitable zone: the Kepler Mission. In: Sun, Y.-S., Ferraz-Mello,  
574 S., Zhou, J.-L. (Eds.), *IAU Symposium*. Vol. 249 of *IAU Symposium*. pp.  
575 17–24.
- 576 Brown, T. M., Gilliland, R. L., Noyes, R. W., Ramsey, L. W., Feb. 1991.  
577 Detection of possible p-mode oscillations on Procyon. *ApJ* 368, 599–609.
- 578 Buzasi, D., Catanzarite, J., Laher, R., et al., Apr. 2000. The Detection of  
579 Multimodal Oscillations on  $\alpha$  Ursae Majoris. *ApJ* 532, L133–L136.
- 580 Carrier, F., Bourban, G., Jul. 2003. Solar-like oscillations in the K1 dwarf  
581 star alpha Cen B. *A&A* 406, L23–L26.
- 582 Carrier, F., De Ridder, J., Baudin, F., et al., Jan. 2010. Non-radial oscilla-  
583 tions in the red giant HR 7349 measured by CoRoT. *A&A* 509, A73.
- 584 Carter, J. A., Agol, E., Chaplin, W. J., et al., Aug. 2012. Kepler-36: A Pair  
585 of Planets with Neighboring Orbits and Dissimilar Densities. *Science* 337,  
586 556.

- 587 Chaplin, W. J., Appourchaux, T., Elsworth, Y., et al., Apr. 2010. The As-  
588 teroseismic Potential of Kepler: First Results for Solar-Type Stars. *ApJ*  
589 713, L169–L175.
- 590 Chaplin, W. J., Kjeldsen, H., Christensen-Dalsgaard, J., et al., Apr. 2011.  
591 Ensemble Asteroseismology of Solar-Type Stars with the NASA Kepler  
592 Mission. *Science* 332, 213.
- 593 Chaplin, W. J., Miglio, A., Mar. 2013. Asteroseismology of Solar-Type and  
594 Red-Giant Stars. *ArXiv e-prints*: 1303.1957.
- 595 Chaplin, W. J., Sanchis-Ojeda, R., Campante, T. L., et al., Apr. 2013. Aster-  
596 oseismic Determination of Obliquities of the Exoplanet Systems Kepler-50  
597 and Kepler-65. *ApJ* 766, 101.
- 598 Christensen-Dalsgaard, J., Apr. 2004. Physics of solar-like oscillations. *Solar*  
599 *Physics* 220, 137–168.
- 600 Christensen-Dalsgaard, J., Aug. 2008. ASTEC - the Aarhus STellar Evolution  
601 Code. *Ap&SS* 316, 13–24.
- 602 Christensen-Dalsgaard, J., Jun. 2011. Asteroseismology of red giants. *ArXiv*  
603 *e-prints*: 1106.5946.
- 604 Christensen-Dalsgaard, J., Dec. 2012. Stellar model fits and inversions. *As-*  
605 *tronomische Nachrichten* 333, 914.
- 606 Córscico, A. H., Althaus, L. G., Miller Bertolami, M. M., Bischoff-Kim, A.,  
607 May 2012. Asteroseismology of the Kepler V777 Herculis variable white  
608 dwarf with fully evolutionary models. *A&A* 541, A42.
- 609 De Ridder, J., Barban, C., Baudin, F., et al., May 2009. Non-radial oscillation  
610 modes with long lifetimes in giant stars. *Nature* 459, 398–400.
- 611 De Ridder, J., Barban, C., Carrier, F., et al., Mar. 2006. Discovery of solar-  
612 like oscillations in the red giant  $\epsilon$  Ophiuchi. *A&A* 448, 689–695.
- 613 Degroote, P., Aerts, C., Baglin, A., et al., Mar. 2010. Deviations from a  
614 uniform period spacing of gravity modes in a massive star. *Nature* 464,  
615 259–261.

- 616 Deheuvels, S., García, R. A., Chaplin, W. J., et al., Sep. 2012. Seismic Evi-  
617 dence for a Rapidly Rotating Core in a Lower-giant-branch Star Observed  
618 with Kepler. *ApJ* 756, 19.
- 619 Deheuvels, S., Michel, E., Jul. 2010. New insights on the interior of solar-like  
620 pulsators thanks to CoRoT: the case of HD 49385. *Ap&SS* 328, 259–263.
- 621 Deheuvels, S., Michel, E., Nov. 2011. Constraints on the structure of the core  
622 of subgiants via mixed modes: the case of HD 49385. *A&A* 535, A91.
- 623 Deng, L., Xin, Y., Zhang, X., et al., Jan. 2013. SONG China project - partic-  
624 ipating in the global network. In: Burton, M. G., Cui, X., Tothill, N. F. H.  
625 (Eds.), *IAU Symposium*. Vol. 288 of *IAU Symposium*. pp. 318–319.
- 626 Dupret, M.-A., Belkacem, K., Samadi, R., et al., Oct. 2009. Theoretical  
627 amplitudes and lifetimes of non-radial solar-like oscillations in red giants.  
628 *A&A* 506, 57–67.
- 629 Dziembowski, W. A., Gough, D. O., Houdek, G., Sienkiewicz, R., Dec. 2001.  
630 Oscillations of  $\alpha$  UMa and other red giants. *MNRAS* 328, 601–610.
- 631 Frandsen, S., Carrier, F., Aerts, C., et al., Oct. 2002. Detection of Solar-like  
632 oscillations in the G7 giant star  $\xi$  Hya. *A&A* 394, L5–L8.
- 633 García, R. A., Mathur, S., Ballot, J., et al., Sep. 2008. Influence of Low-  
634 Degree High-Order p-Mode Splittings on the Solar Rotation Profile. *SoPh*  
635 251, 119–133.
- 636 García, R. A., Régulo, C., Samadi, R., et al., Oct. 2009. Solar-like oscillations  
637 with low amplitude in the CoRoT target HD 181906. *A&A* 506, 41–50.
- 638 García, R. A., Turck-Chièze, S., Jiménez-Reyes, S. J., et al., Jun. 2007.  
639 Tracking Solar Gravity Modes: The Dynamics of the Solar Core. *Science*  
640 316, 1591–.
- 641 Gaulme, P., Deheuvels, S., Weiss, W. W., et al., Dec. 2010. HD 46375: seis-  
642 mic and spectropolarimetric analysis of a young Sun hosting a Saturn-like  
643 planet. *A&A* 524, A47.
- 644 Gilliland, R. L., Jenkins, J. M., Borucki, W. J., et al., Apr. 2010. Initial  
645 Characteristics of Kepler Short Cadence Data. *ApJ* 713, L160–L163.

- 646 Girardi, L., Groenewegen, M. A. T., Hatziminaoglou, E., da Costa, L., Jun.  
647 2005. Star counts in the Galaxy. Simulating from very deep to very shallow  
648 photometric surveys with the TRILEGAL code. *A&A* 436, 895–915.
- 649 Gizon, L., Solanki, S. K., Jun. 2003. Determining the Inclination of the  
650 Rotation Axis of a Sun-like Star. *ApJ* 589, 1009–1019.
- 651 Goldreich, P., Keeley, D. A., Feb. 1977. Solar seismology. II - The stochastic  
652 excitation of the solar p-modes by turbulent convection. *ApJ* 212, 243–251.
- 653 Goldreich, P., Kumar, P., Mar. 1988. The interaction of acoustic radiation  
654 with turbulence. *ApJ* 326, 462–478.
- 655 Gough, D. O., 1986. Solar and solar-like oscillations - Theory. *Highlights of*  
656 *Astronomy* 7, 283–293.
- 657 Gough, D. O., 1990. Comments on Helioseismic Inference. In: Osaki, Y.,  
658 Shibahashi, H. (Eds.), *Progress of Seismology of the Sun and Stars*. Vol.  
659 367 of *Lecture Notes in Physics*, Berlin Springer Verlag. p. 283.
- 660 Hekker, S., Aerts, C., De Ridder, J., Carrier, F., Nov. 2006. Pulsations de-  
661 tected in the line profile variations of red giants. Modelling of line moments,  
662 line bisector and line shape. *A&A* 458, 931–940.
- 663 Hekker, S., Arentoft, T., Kjeldsen, H., et al., Oct. 2008. Oscillations in Pro-  
664 cyon A: First results from a multi-site campaign. *Journal of Physics Con-*  
665 *ference Series* 118 (1), 012059.
- 666 Hekker, S., Broomhall, A.-M., Chaplin, W. J., et al., Mar. 2010. The Octave  
667 (Birmingham-Sheffield Hallam) automated pipeline for extracting oscilla-  
668 tion parameters of solar-like main-sequence stars. *MNRAS* 402, 2049–2059.
- 669 Hekker, S., Elsworth, Y., De Ridder, J., et al., Jan. 2011. Solar-like oscilla-  
670 tions in red giants observed with Kepler: comparison of global oscillation  
671 parameters from different methods. *A&A* 525, A131.
- 672 Hekker, S., Elsworth, Y., Mosser, B., et al., Aug. 2012. Solar-like oscillations  
673 in red giants observed with Kepler: influence of increased timespan on  
674 global oscillation parameters. *A&A* 544, A90.

- 675 Hekker, S., Kallinger, T., Baudin, F., et al., Oct. 2009. Characteristics of  
676 solar-like oscillations in red giants observed in the CoRoT exoplanet field.  
677 *A&A* 506, 465–469.
- 678 Howell, S. B., Rowe, J. F., Bryson, S. T., et al., Feb. 2012. Kepler-21b: A  
679  $1.6 R_{Earth}$  Planet Transiting the Bright Oscillating F Subgiant Star HD  
680 179070. *ApJ* 746, 123.
- 681 Huber, D., Bedding, T. R., Arentoft, T., et al., Apr. 2011. Solar-like Oscil-  
682 lations and Activity in Procyon: A Comparison of the 2007 MOST and  
683 Ground-based Radial Velocity Campaigns. *ApJ* 731, 94.
- 684 Huber, D., Bedding, T. R., Stello, D., et al., Nov. 2010. Asteroseismology of  
685 Red Giants from the First Four Months of Kepler Data: Global Oscillation  
686 Parameters for 800 Stars. *ApJ* 723, 1607–1617.
- 687 Huber, D., Chaplin, W. J., Christensen-Dalsgaard, J., et al., Apr. 2013.  
688 Fundamental Properties of Kepler Planet-candidate Host Stars using As-  
689 teroseismology. *ApJ* 767, 127.
- 690 Huber, D., Stello, D., Bedding, T. R., et al., Oct. 2009. Automated extrac-  
691 tion of oscillation parameters for Kepler observations of solar-type stars.  
692 *Communications in Asteroseismology* 160, 74.
- 693 Kaiser, A., Kuschnig, R., Weiss, W. W., BRITE-Constellation Team, Dec.  
694 2012. Brite-Constellation: A status report. *Astronomische Nachrichten*  
695 333, 1096.
- 696 Kallinger, T., Mosser, B., Hekker, S., et al., Nov. 2010. Asteroseismology of  
697 red giants from the first four months of Kepler data: Fundamental stellar  
698 parameters. *A&A* 522, A1.
- 699 Kawaler, S. D., Reed, M. D., Quint, A. C., et al., Dec. 2010. First Kepler re-  
700 sults on compact pulsators - II. KIC 010139564, a new pulsating subdwarf  
701 B (V361 Hya) star with an additional low-frequency mode. *MNRAS* 409,  
702 1487–1495.
- 703 Kjeldsen, H., Bedding, T. R., Jan. 1995. Amplitudes of stellar oscillations:  
704 the implications for asteroseismology. *A&A* 293, 87–106.

- 705 Kjeldsen, H., Bedding, T. R., Viskum, M., Frandsen, S., Mar. 1995. Solarlike  
706 oscillations in eta Boo. *AJ* 109, 1313–1319.
- 707 Kolenberg, K., Szabó, R., Kurtz, D. W., et al., Apr. 2010. First Kepler  
708 Results on RR Lyrae Stars. *ApJ* 713, L198–L203.
- 709 Léger, A., Rouan, D., Schneider, J., et al., Oct. 2009. Transiting exoplanets  
710 from the CoRoT space mission. VIII. CoRoT-7b: the first super-Earth  
711 with measured radius. *A&A* 506, 287–302.
- 712 Lopes, I., Turck-Chieze, S., Oct. 1994. The second order asymptotic theory  
713 for the solar and stellar low degree acoustic mode predictions. *A&A* 290,  
714 845–860.
- 715 Mathur, S., García, R. A., Régulo, C., et al., Feb. 2010. Determining global  
716 parameters of the oscillations of solar-like stars. *A&A* 511, A46.
- 717 Mathur, S., Handberg, R., Campante, T. L., et al., Jun. 2011a. Solar-like  
718 Oscillations in KIC 11395018 and KIC 11234888 from 8 Months of Kepler  
719 Data. *ApJ* 733, 95.
- 720 Mathur, S., Hekker, S., Trampedach, R., et al., Nov. 2011b. Granulation in  
721 Red Giants: Observations by the Kepler Mission and Three-dimensional  
722 Convection Simulations. *ApJ* 741, 119.
- 723 Mathur, S., Metcalfe, T. S., Woitaszek, M., et al., Apr. 2012. A Uniform  
724 Asteroseismic Analysis of 22 Solar-type Stars Observed by Kepler. *ApJ*  
725 749, 152.
- 726 Matthews, J. M., Kuschnig, R., Walker, G. A. H., et al., 2000. Ultraprecise  
727 Photometry from Space: The MOST Microsat Mission. In: Szabados, L.,  
728 Kurtz, D. (Eds.), *IAU Colloq. 176: The Impact of Large-Scale Surveys on*  
729 *Pulsating Star Research*. Vol. 203 of *Astronomical Society of the Pacific*  
730 *Conference Series*. pp. 74–75.
- 731 Mazumdar, A., Mérand, A., Demarque, P., et al., Aug. 2009. Asteroseis-  
732 mology and interferometry of the red giant star  $\epsilon$  Ophiuchi. *A&A* 503,  
733 521–531.
- 734 Mazumdar, A., Michel, E., Antia, H. M., Deheuvels, S., Apr. 2012a. Seismic  
735 detection of acoustic sharp features in the CoRoT target HD 49933. *A&A*  
736 540, A31.

- 737 Mazumdar, A., Monteiro, M. J. P. F. G., Ballot, J., et al., Dec. 2012b. Acous-  
738 tic glitches in solar-type stars from Kepler. *Astronomische Nachrichten* 333,  
739 1040–1043.
- 740 Metcalfe, T. S., Chaplin, W. J., Appourchaux, T., et al., Mar. 2012. Astero-  
741 seismology of the Solar Analogs 16 Cyg A and B from Kepler Observations.  
742 *ApJ* 748, L10.
- 743 Michel, E., Baglin, A., Auvergne, M., et al., Oct. 2008. CoRoT Measures  
744 Solar-Like Oscillations and Granulation in Stars Hotter Than the Sun.  
745 *Science* 322, 558.
- 746 Miglio, A., Montalbán, J., Baudin, F., et al., Sep. 2009. Probing populations  
747 of red giants in the galactic disk with CoRoT. *A&A* 503, L21–L24.
- 748 Miglio, A., Montalbán, J., Carrier, F., et al., Sep. 2010. Evidence for a sharp  
749 structure variation inside a red-giant star. *A&A* 520, L6.
- 750 Mosser, B., Appourchaux, T., Dec. 2009. On detecting the large separation  
751 in the autocorrelation of stellar oscillation times series. *A&A* 508, 877–887.
- 752 Mosser, B., Barban, C., Montalbán, J., et al., Aug. 2011a. Mixed modes in  
753 red-giant stars observed with CoRoT. *A&A* 532, A86.
- 754 Mosser, B., Belkacem, K., Goupil, M.-J., et al., Jul. 2010. Red-giant seismic  
755 properties analyzed with CoRoT. *A&A* 517, A22.
- 756 Mosser, B., Belkacem, K., Goupil, M. J., et al., Jan. 2011b. The universal  
757 red-giant oscillation pattern. An automated determination with CoRoT  
758 data. *A&A* 525, L9.
- 759 Mosser, B., Goupil, M. J., Belkacem, K., et al., Dec. 2012. Spin down of the  
760 core rotation in red giants. *A&A* 548, A10.
- 761 Prša, A., Batalha, N., Slawson, R. W., et al., Mar. 2011. Kepler Eclipsing  
762 Binary Stars. I. Catalog and Principal Characterization of 1879 Eclipsing  
763 Binaries in the First Data Release. *AJ* 141, 83.
- 764 Rauer, H., Sep. 2012. The PLATO Mission. In: *European Planetary Science*  
765 *Congress 2012*. p. 415.

- 766 Roxburgh, I. W., May 2005. The ratio of small to large separations of stellar  
767 p-modes. *A&A* 434, 665–669.
- 768 Roxburgh, I. W., Vorontsov, S. V., Nov. 2003. The ratio of small to large  
769 separations of acoustic oscillations as a diagnostic of the interior of solar-  
770 like stars. *A&A* 411, 215–220.
- 771 Schrijvers, C., Telting, J. H., Aerts, C., et al., Feb. 1997. Line-profile varia-  
772 tions due to adiabatic non-radial pulsations in rotating stars. I. Observable  
773 characteristics of spheroidal modes. *A&AS* 121, 343–368.
- 774 Stello, D., Chaplin, W. J., Basu, S., et al., Nov. 2009. The relation between  
775  $\Delta\nu$  and  $\nu_{max}$  for solar-like oscillations. *MNRAS* 400, L80–L84.
- 776 Stello, D., Kjeldsen, H., Bedding, T. R., Buzasi, D., Mar. 2006. Oscillation  
777 mode lifetimes in  $\xi$  Hydrae: will strong mode damping limit asteroseismol-  
778 ogy of red giant stars? *A&A* 448, 709–715.
- 779 Tassoul, M., Aug. 1980. Asymptotic approximations for stellar nonradial  
780 pulsations. *ApJS* 43, 469–490.
- 781 Torra, J., Gaia group, May 2013. Gaia: the challenge begins. In: *Highlights*  
782 *of Spanish Astrophysics VII*. pp. 82–94.
- 783 Ulrich, R. K., Jul. 1986. Determination of stellar ages from asteroseismology.  
784 *ApJ* 306, L37–L40.
- 785 Uytterhoeven, K., Moya, A., Grigahcène, A., et al., Oct. 2011. The Kepler  
786 characterization of the variability among A- and F-type stars. I. General  
787 overview. *A&A* 534, A125.
- 788 Uytterhoeven, K., Pallé, P. L., Grundahl, F., et al., Dec. 2012. SONG-OT:  
789 The prototype SONG node at Tenerife. *Astronomische Nachrichten* 333,  
790 1103–1106.
- 791 Ventura, P., D’Antona, F., Mazzitelli, I., Aug. 2008. The ATON 3.1 stellar  
792 evolutionary code. A version for asteroseismology. *Ap&SS* 316, 93–98.
- 793 Verner, G. A., Elsworth, Y., Chaplin, W. J., et al., Aug. 2011. Global aster-  
794 oseismic properties of solar-like oscillations observed by Kepler: a compar-  
795 ison of complementary analysis methods. *MNRAS* 415, 3539–3551.

- 796 Vorontsov, S. V., 1988. A Search of the Effects of Magnetic Field in the So-  
797 lar 5-MINUTE Oscillations. In: Christensen-Dalsgaard, J., Frandsen, S.  
798 (Eds.), *Advances in Helio- and Asteroseismology*. Vol. 123 of IAU Sympo-  
799 sium. p. 151.
- 800 Wagner, F. W., Tosi, N., Sohl, F., et al., May 2012. Rocky super-Earth  
801 interiors. Structure and internal dynamics of CoRoT-7b and Kepler-10b.  
802 *A&A* 541, A103.
- 803 White, T. R., Bedding, T. R., Gruberbauer, M., et al., Jun. 2012. Solving  
804 the Mode Identification Problem in Asteroseismology of F Stars Observed  
805 with Kepler. *ApJ* 751, L36.
- 806 Zwintz, K., Fossati, L., Ryabchikova, T., et al., Feb. 2013.  $\gamma$  Doradus pul-  
807 sation in two pre-main sequence stars discovered by CoRoT. *A&A* 550,  
808 A121.